Improving the performance of damage repair in thin-walled structures with analytical data and machine learning algorithms

Abdul Aabid
Department of Engineering Management, College of Engineering,
Prince Sultan University, PO BOX 66833, Riyadh 11586, Saudi Arabia

Md Abdul Raheman
NITTE (Deemed to be University), Dept. of Electrical and Electronics Engineering,
NMAM Institute of Technology, Nitte - 574110, Karnataka, India

Meftah Hrairi*
Department of Mechanical and Aerospace Engineering, Faculty of Engineering,
International Islamic University Malaysia, P.O. Box 10, 50725 Kuala Lumpur, Malaysia

Muneer Baig
Department of Engineering Management, College of Engineering,
Prince Sultan University, PO BOX 66833, Riyadh 11586, Saudi Arabia

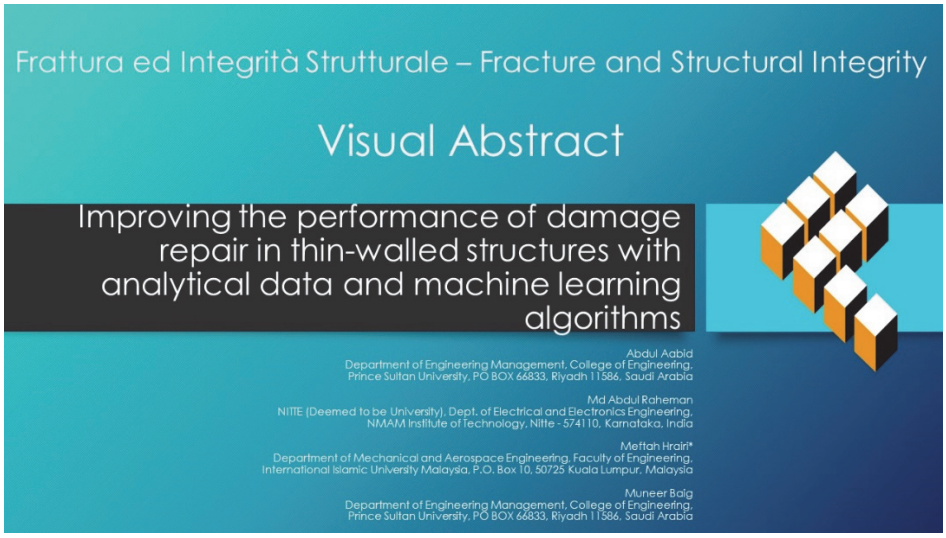

Citation: Aabid, A., Raheman, M. A., Hrairi, M., Baig, M., Improving the performance of damage repair in thin-walled structures with analytical data and machine learning algorithms, Frattura ed Integrità Strutturale, 68 (2024) 310-324.

Received: 31.01.2024
Accepted: 27.02.2024
Published: 05.03.2024
Issue: 04.2024

KEYWORDS. Bonded composite repair, Cracks, Reinforced patch, Analytical model; Machine learning.

INTRODUCTION

Composite materials, known for their lightweight and high strength, are extensively utilized in high-performance engineering applications. These materials play a crucial role in the aerospace industry, constituting approximately 80% of aircraft structures. Over the past four decades, composite materials have been employed in repairing various structures, such as plates, pipes, shells, and trusses, proving to be a cost-effective alternative to replacing the entire structure. In aircraft structures, damage is a critical concern, often necessitating the replacement of the entire component. To address this, researchers have leveraged advanced composite materials to repair damages, presenting a highly effective method for addressing cracks. Numerous studies, employing experimental, numerical, and mathematical approaches, have demonstrated the effectiveness of using composite materials for repairing cracked structures. The current study reviews relevant research to establish the novelty of its approach.

Composite patches, when bonded onto cracked or corroded metallic aircraft structures, offer a cost-effective solution for extending service life and maintaining structural efficiency [1–4]. The design of aircraft structures requires diligent inspection and monitoring of defects at regular intervals to ensure damage tolerance and fail-safe operation. The replacement of damaged structural components significantly impacts the life cycle cost of an airplane. In recent years, bonded composite patches have gained widespread use for repairing cracks and defects in aircraft structures [5–7]. This technology provides several advantages over traditional methods such as mechanical fastening or riveting, including improved fatigue behavior, restored stiffness and strength, reduced corrosion, and the ability to be readily formed into complex shapes.

The use of composite patches for repairing cracked plates has been extensively investigated, with researchers exploring different shapes and variations to improve repair performance [8,9]. Composite patches have been utilized by varying parameters, as demonstrated in studies conducted by Aabid et al. [10]. Recent studies have adopted a design of experiments (DOE) approach to investigate the effect of material properties and dimensions on repair performance, to reduce computational and experimental time [11]. The hybridization of multiple volume fractions of fibers in composite patches of varying stiffness has been studied to identify optimal parameters for minimizing SIF [12]. The lamina composite patch has significant effect while having the fiber direction perpendicular to the crack length and this has been proved through the finite element (FE) simulations [13]. In addition, a hybrid repair technique that involved bonded and drilled holes was used to demonstrate repair performance in aircraft structures using elastoplastic analysis [14]. The bonded composite repair method has been extensively demonstrated through the FE approach over the last four decades considering all possible aspects of the problem definition [15]. However, it has been stated that the mathematical modelling lacks parametric information, and it can be considered with limited parameters from the problem definition [16,17].

In recent years, soft computing tools have become increasingly popular in various engineering fields for predicting and solving optimum results. ML algorithms are particularly useful in applications where clear concepts cannot be obtained from experimentation data [18,19]. In mechanical engineering, numerous studies have reported using ML algorithms, and some technical approaches to simplify mechanical problems can be found in the review work of Nasiri et al. [20]. They explored diverse artificial intelligence methods, including fuzzy logic, Bayesian networks, genetic algorithms, and artificial neural networks, to address fracture mechanics issues. Wang et al. [21] introduced a fatigue crack growth calculation approach utilizing ML algorithms like the extreme learning machine. Rovinelli et al. [22] employed an ML algorithm combined with the Bayesian network to forecast variables such as micro-mechanical and micro-structural factors influencing fatigue crack propagation direction and rate. Balcloglu et al. [23] employed six artificial neural network algorithms to optimize solutions for adhesively bonded pultruded failure loads. Atilla et al. [24] utilized the Levenberg–Marquardt backpropagation algorithm for predicting the buckling load and natural frequency of laminated composites. Lastly, Simsek et al. [25] conducted damage detection in anisotropic-laminated composite beams based on incomplete modal data and teaching–learning-based optimization. The above works show the effectiveness of using a soft-computing approach and slight sign for new researchers to utilize these technologies for enhancing repair performance.

After conducting a critical review of bonded composite repairs for mode-1 crack propagation, it was discovered that various types of patch materials were used to enhance repair performance. Furthermore, patch dimensions and shapes were varied for the same region. Despite this research and the authors' knowledge from the past four decades, attention has not been given to the influence of the ML algorithms with the use of analytical data on the repair of cracked plates for mode-I crack propagation. Thus, the primary contribution of the current work is to identify the effectiveness of parameters to mitigate the SIF to enhance bonded composite repair performance through ML algorithms. To conduct this study calculated a training dataset connecting the patch and adhesive parameters for the SIF using the analytical model (Eqn. 2) and compare

different regression ML models to approximate these data for the accuracy of the results to enhance the bonded repair performance.

PROBLEM FORMULATION

Based on Fig. 1, the focus is on a center-cracked plate with a crack length of 2a, repaired by a bonded composite strip of height 2H across a width of 2W. A uniform tensile stress σ_0 is applied to the plate perpendicular to the crack. The objective is to mitigate the SIF in the repaired plate, considering the crack length and relevant parameters of the patched system, such as thickness, width, height, adhesive thickness, and shear modulus. The subscripts P and A distinguish properties related to the patch and adhesive layer. Due to the bending moment in the repaired region, stress, strain, and displacement vary through the plate thickness, causing the SIF to vary across the crack front. According to Reissner's [26] shear deformation theory for plates, the crack tip singular field for a cracked plate under membrane and bending stresses has the same functional form as a plate under extensional load only [27–29], with the SIF linearly varying through the plate thickness. This implies that the y-stress at position r ahead of the crack tip is described in Wang et al. [29] analytical investigation.

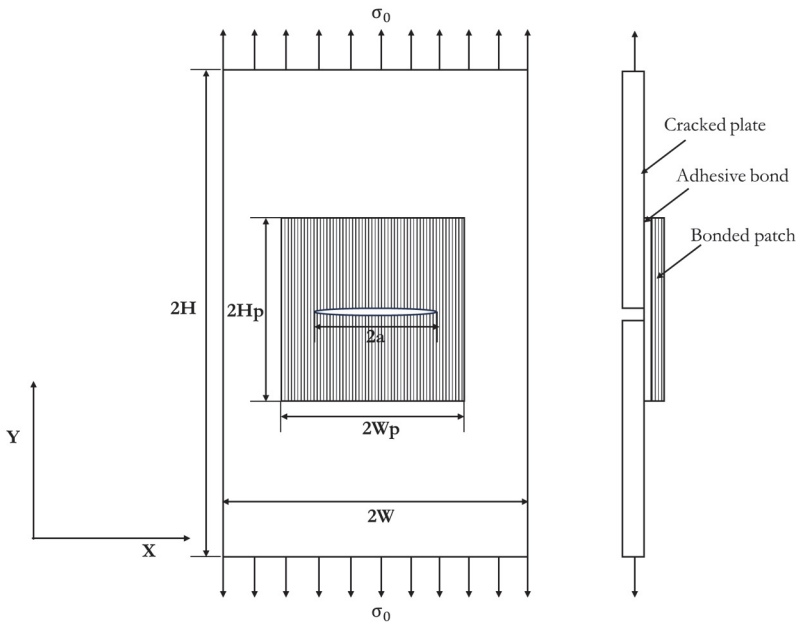

Figure 1: Geometrical model of the patched structure.

Referring to materials of plate, patch, and adhesive bond this investigation used aluminium 2024-T3, reinforced composite, and Araldite 2014 respectively. The properties given for the cracked plate are a density of 2715 kg/m^3, Poisson's ratio of 0.33, and Young's modulus of 68.95 GPa with dimensions of 200 mm of height, 40 mm of width, and 1 mm of thickness. Whereas the reinforced composite has the Poisson's ratio = 0.35, Young's modulus = 16.68 GPA, and shear modulus = 2.56 GPA with the dimensions are 20 mm in height/width and 0.5 mm in thickness. The plate contains a crack length of 20 mm at the central and a composite patch bonded fully on the cracked area using the Araldite 2014 adhesive bond. The properties of the adhesive bond are a density of 1160 kg/m^3, Poisson's ratio of 0.345, Young's modulus of 5.1 GPa, and shear modulus is 1.2 GPa with dimensions are 20 mm of height/width and 0.03 mm of thickness. Fig. 1 illustrates the complete model for the analytical investigation.

ANALYTICAL MODELLING

Unrepaired plate (theoretical formula)

A prior study in fracture mechanics has established a formula within the framework of linear elastic fracture mechanics (LEFM) to compute the SIF for an infinite fractured plate. The SIF characterizes stress distribution at the crack tip in a linear elastic material, with σ_0 representing the uniaxial tensile load perpendicular to the crack

length. In the perspective of a finite plate, boundary conditions lead to elevated stress at the crack tip. The study specifically addresses the mode-I (opening) SIF for a center-cracked plate [30],

$$K_I = \sigma_0 \sqrt{\pi a}\ F\left(\frac{a}{W}\right) = \sigma_0 \sqrt{\pi a}\left[\sec\frac{\pi a}{2W}\right]^{1/2}\left[1-0.025\left(\frac{a}{W}\right)^2+0.06\left(\frac{a}{W}\right)^4\right] \quad (1)$$

Repaired plate (previous study)

The passive reinforcement impact from a reinforced composite patch on a cracked plate under uniform uniaxial tensile stress, σ_0, can be likened to a diminished uniform tension stress, σ_p, exerted on the bonded surface of the cracked plate. This equivalence is achieved through the application of the superposition principle [31,32].In the case of an infinite plate addressing the fundamental crack problem within the LEFM, the solution is derived from Eqn. (2), extensively elaborated by Aabid et al. [5]. The significance of the geometry factor function F(a/w) arises when the crack length is impacted by the geometry of the crack body. To account for this, the equation is reformulated using the empirical formula suggested by Tada et al. [30] for a finite center-cracked rectangular plate, resulting in the following expression:

$$K_I = \delta_1\delta_2.\sigma_p\sqrt{\pi a}\left[sec\frac{\pi a}{2W}\right]^{1/2}\left[1-0.025\left(\frac{a}{W}\right)^2+0.06\left(\frac{a}{W}\right)^4\right] \quad (2)$$

where

$$\delta_1 = \frac{1}{1+S}; \qquad \delta_2 = \sqrt{\frac{c}{a+c}}$$

and

$$c = \frac{(1+S)}{S}.\frac{\left(1-\nu^2\right)}{\pi\beta}$$

where S is the stiffness ratio between the composite patch and crack plate, ν is the Poisson's ratio (plate), and β is shear stress transfer length in a representative bonded joint. In comparison to the SIF solution for an infinite center-cracked aluminium plate, the composite reinforcement effect is considered by introducing two correction factors, namely δ_1 and δ_2 [5]. Both correction factors, with values less than one, indicate that incorporating composite reinforcement in the center-cracked aluminium plate leads to a reduction in SIFs. The reinforcing impact of composite patches primarily stems from alleviating stress and constraints on the crack opening [31,32].

MACHINE LEARNING

Machine Learning (ML) is a component of artificial intelligence built on the concept that machines can learn from data, identify patterns, and make decisions with minimal human involvement. It serves as a data analysis method that automates the development of analytical models. Depending on the training data, different learning models have been developed. Regression techniques, a form of supervised ML techniques, are used for predictive modelling and data mining tasks. Regression techniques encompass a wide range of learning techniques each with its own set of benefits and drawbacks. This complicates the selection of the best model for a given data.

In the current work, the problem is defined based on the plate, adhesive and patch hence the parameter selected from the dimensions and mechanical properties to perform ML work. Since the purpose of this study is to interpolate the limited data, the regression techniques will be utilized as an ML approach. The techniques used in this paper are: Ordinary Least Squares (OLS), Ridge, Lasso, Elastic Net, k Nearest Neighbours (kNN), Decision Tree (DT), Random Forest (RF) and Support Vector Machine (SVM) techniques. Python programming language was used to create the scripts. The ML process shown in Fig. 2 was carried out using the scikit-learn library.

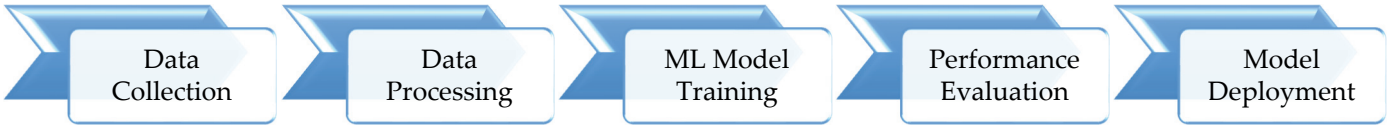

Figure 2: Machine learning process.

Data set and properties

In this research, the numerical exploration focused on the influence of crack length, composite patch dimensions, and adhesive bond on the SIF. The dataset encompasses 6 features and 1 target value. Tab. 1(a) details that feature X1 denotes the crack length, while features X2, X3, and X4 represent the thickness, width, and height of the composite patch, respectively. Additionally, features X5 and X6 correspond to the thickness and shear modulus of the adhesive bond. Y1 serves as the target parameter, calculated through ML techniques, and signifies the SIF. These characteristics, along with the target value, are outlined in Tab. 1(a). The data set contains 19 data points from numerical studies as shown in Fig 3. The range of each parameter was chosen based on the existing work in this field. It has been stated that the maximum variation of the bonded composite repair parameters is suitable for the range considered in this work and it can influence the mitigation of SIF which we can see in the result section [10,11,33].

Feature Id	Property	Range	Data Type
X1	Crack Length	5 – 15 mm	Numeric
X2	Patch Thickness	0.5 – 1 mm	Numeric
X3	Patch Width	17.5 – 22.5 mm	Numeric
X4	Patch Height	10 – 12.5 mm	Numeric
X5	Adhesive Thickness	0.0025 – 0.0035 mm	Numeric
X6	Shear Modulus	0.6 – 1.8 GPa	Numeric

Table 1(a): Numerical analysis data set and their properties.

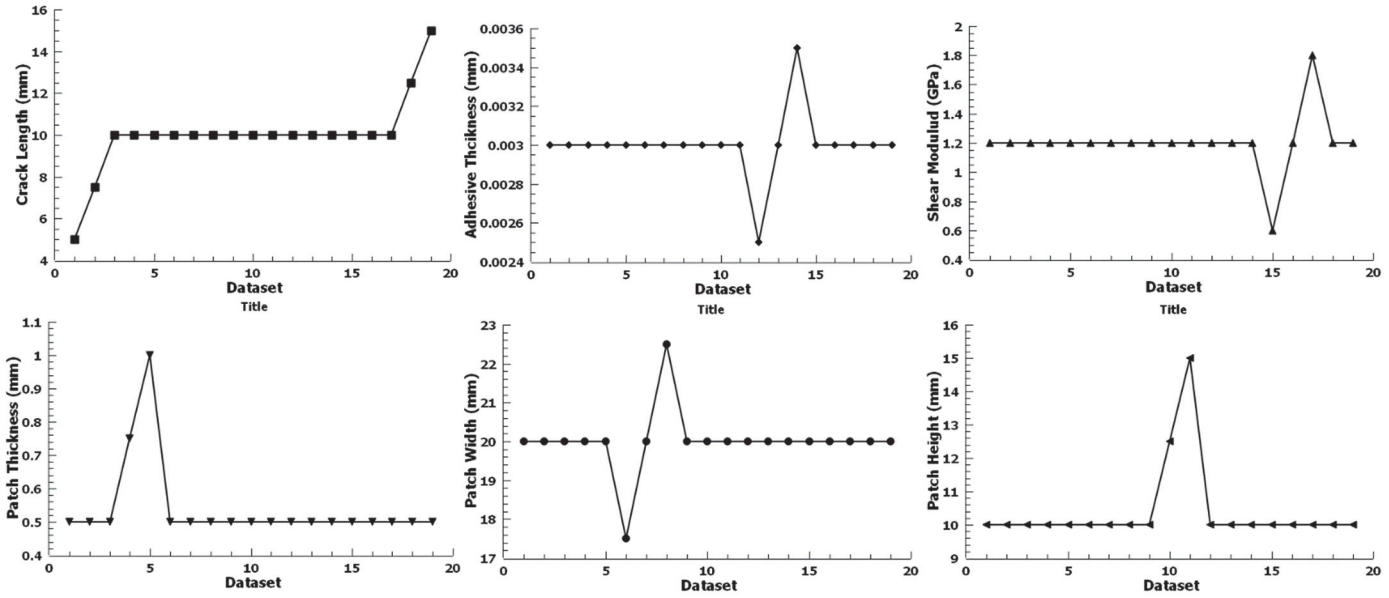

Figure 3: Value of various features in 19 datapoints of dataset.

A correlation coefficient used in statistics to assess the linear connection between two sets of data is the Pearson correlation coefficient (PCC) given in Eqn. (3), where r_{xy} is the correlation coefficient between x and y variables; x_i are values of the x-variable in a sample; $\overline{x}$ is mean of the values of the x-variables; y_i are values of y-variable in a sample; and $\overline{y}$ is mean of the values of the y-variable. It is effectively a normalized measurement of covariance since it is the ratio of two variables'

covariance to the product of their standard deviations; as a result, the result is always between −1 and 1. A linear equation with all data points falling on a line that precisely characterizes the connection between X and Y is implied by an absolute value of 1. A regression slope value of +1 indicates that all data points are on a line where Y rises as X increases, and vice versa for a value of -1. This indicates the sign of the connection. There is no linear relationship between the variables when the value is 0.

$$r_{xy} = \frac{\sum_{i=1}^{n}(x_i - \bar{x})(y_i - \bar{y})}{\sqrt{\sum_{i=1}^{n}(x_i - \bar{x})^2}\sqrt{\sum_{i=1}^{n}(y_i - \bar{y})^2}} \tag{3}$$

The correlation between various parameters is shown in Tab. 1(b). From Tab. 1(b), NSIF (the ratio of the repaired plate to the healthy plate) is highly dependent on the crack length (X1) and patch thickness (X2). A negative correlation indicates that as one variable value increases, the other decreases. From Tab. 1(b), it is evident that normalized SIF varies linearly with crack length and patchwork, and hence one can utilize linear regression models for the prediction of NSIF.

Parameters	X1	X2	X3	X4	X5	X6	NSIF
X1	1	-	-	-	-	-	-
X2	0	1	-	-	-	-	-
X3	0	0	1	-	-	-	-
X4	0	-0.10465	0	1	-	-	-
X5	0	-4.27E-18	0	1.14E-18	1	-	-
X6	0	-7.69E-18	0	-1.23E-17	-1.60E-31	1	-
NSIF	-0.82863	-0.48607	-0.03608	0.044724	0.010502	-0.08284	1

Table 1(b). Correlation between various parameters.

Machine learning (ML) algorithms

In the field of ML algorithms, there is no single learning algorithm that offers good learning on all real-world challenges. Hence, algorithm selection was done based on the existing work [34] and the study employed a variety of ML algorithms.

Regression models

A regression model is a statistical approach used to analyze the relationship between one or more independent variables and a dependent variable. It aims to predict or explain the value of the dependent variable by fitting a mathematical equation to observed data points, enabling the estimation of future outcomes. In this work, four different regression models were utilized and can be seen with their mathematical relation in Tab. 2, Here $X\beta - y_2^2$ represents the squared Euclidean norm of the difference between the predicted and actual outcomes, X is the matrix of input features, β is a vector of coefficients, and y is the vector of actual outcomes. α is a regularization parameter in Ridge, Lasso, and Elastic Net regressions that controls the strength of penalty applied to coefficients. β_2^2 represents the squared Euclidean norm of coefficient vector β in Ridge Regression. β_1 represents the L1 norm (or Manhattan distance) of coefficient vector β in Lasso Regression. In Elastic Net Regression, ρ parameter balances between Ridge (L2) and Lasso (L1) penalties. When $\rho = 0$, it's equivalent to Ridge; when $\rho = 1$, it's equivalent to Lasso.

k Nearest Neighbours

The kNN technique is an ML technique that works based on the values of the nearest k neighbour. The kNN technique is a non-parametric technique used for classification and regression tasks. While performing the learning process, the kNN technique first calculates the distance between the individual data in the investigated data set. The distance may be calculated using Euclidian, Manhattan, or Hamming distance functions. Then, for each data set, the mean value of the nearest k Neighbours is computed. The value of k is the kNN technique's only hyperparameter. If the k value is too low, the boundaries flicker, leading to overfitting. Conversely, a too-high k-value results in smoother separation boundaries, causing underfitting. The drawback of the kNN technique is the distance computation procedure, which increases the processing burden as data grows.

S. No.	Regression models	Mathematical equation
1	OLS Regression	$\min_{\beta} X\beta - y_2^2$
2	Ridge Regression	$\min_{\beta} X\beta - y_2^2 + \alpha\beta_2^2$
3	Lasso Regression	$\min_{\beta} \frac{1}{2n_{\text{samples}}} X\beta - y_2^2 + \alpha\beta_1$
4	Elastic Net Regression	$\min_{\beta} \frac{1}{2n_{\text{samples}}} X\beta - y_2^2 + \alpha\rho\beta_1 + \frac{\alpha(1-\rho)}{2}\beta_2^2$

Table 2: Regression models.

Decision Tree

Decision trees (DT) represent versatile non-parametric supervised ML techniques capable of handling both classification and regression tasks. The primary aim of a DT is to create a model that predicts the target variables' value by learning straightforward decision rules derived from the data features. The DT process involves three key steps. Firstly, the most crucial feature is positioned as the initial node. Next, in the second step, the dataset is divided into subgroups based on this node, with subsets formed using data sharing the same value for each feature. This process is iterated until the final nodes appear in all branches during the third step. The outcome of the technique resembles a root with decision leafs. DT can accommodate both categorical and numerical data.

Support Vector Regression (SVR)

Support vector machine (SVM) is a versatile technique that not only does linear and non-linear classification but also supports regression. The SVR is the SVM technique for regression. SVR aims to fit as many instances on the street as feasible while limiting margin violations. The hyperparameter ε controls the width of the street. SVR has different kernels. Tab. 3 lists some of the most used kernels. Here $\mathbf{a},\mathbf{b}$ are input vectors, γ is a coefficient for the kernel functions, r is a coefficient used in Polynomial and Sigmoid kernels, and d is the degree of the polynomial in Polynomial kernel.

Name of kernel	Kernel function
Linear	$K(\mathbf{a},\mathbf{b}) = \mathbf{a}^T\mathbf{b}$
Polynomial	$K(\mathbf{a},\mathbf{b}) = \left(\gamma\mathbf{a}^T\mathbf{b} + r\right)^d$
Gaussian RBF (Radial basis function)	$K(\mathbf{a},\mathbf{b}) = \exp\left(-\gamma\mathbf{a} - \mathbf{b}^2\right)$
Sigmoid	$K(\mathbf{a},\mathbf{b}) = \tanh\left(\gamma\mathbf{a}^T\mathbf{b} + r\right)$

Table 3: Different kernels of SVR.

Tab. 4 lists the various hyperparameters of various ML techniques used in the study and further the explanation of hyperparameters can be found in [35].

Regression model evaluation and performance metrics

There are many well-known model evaluation techniques such as percentage split and cross-validation. The percentage split is the simplest technique. In this paper, all the data is divided into train and test subsets based on a percentage definition. 80% of the data sample is used for training the model and 20% as the test data. In this paper, the open source scikit learn toolbox is used for the analysis [35]. The training and test subsets are utilized for training and assessing the performance of the model, respectively. The main criteria used for model evaluation and selection of the model are called metrics. The root-mean-square error (RMSE), mean average error (MAE), mean absolute percentage error (MAPE), and coefficient of determination (R^2) are the most widely used regression metrics and are used in this paper. Tab. 5 shows the key equations of performance metrics.

Machine Learning Technique	Parameters
OLS	Hyperparameters: 'copy_X': True, 'fit_intercept': True, 'n_jobs': None, 'normalize': False, 'positive': False Attributes: Coefficients: [[-7.17938824e-03 -1.41997647e-01 -4.48094118e-03 1.34583529e-03 -1.70000000e+00 -1.50833333e-02]] Intercept: [0.53385553
Lasso	Hyperparameters: 'alpha': 0.1, 'copy_X': True, 'fit_intercept': True, 'max_iter': 1000, 'normalize': False, 'positive': False, 'precompute': False, 'random_state':None, 'selection': 'cyclic', 'tol': 0.0001, 'warm_start': False Attributes: Coefficients: [-0.00978855] Intercept: [0.40325331]
Ridge	Hyperparameters: 'alpha': 0.5, 'copy_X': True, 'fit_intercept': True, 'max_iter': None, 'normalize': False, 'random_state':None, 'solver': 'auto', 'tol': 0.001
Elastic Net	Hyperparameters: 'alpha': 0.2, 'copy_X': True, 'fit_intercept': True, 'l1_ratio': 0.5, 'max_iter': 1000, 'normalize': False, 'positive': False, 'precompute': False, 'random_state':None, 'selection': 'cyclic', 'tol': 0.0001, 'warm_start': False Attributes: Coefficients: [-0.00973463] Intercept: [0.40275909]
SVRLIN	Hyperparameters: 'C': 5, 'cache_size': 200, 'coef0': 0.0, 'degree': 3, 'epsilon': 0.01, 'gamma': 'scale', 'kernel': 'linear', 'max_iter': -1, 'shrinking': True, 'tol': 0.001, 'verbose': False
SVRPOLY	Hyperparameters: 'C': 5, 'cache_size': 200, 'coef0': 0.0, 'degree': 3, 'epsilon': 0.01, 'gamma': 'scale', 'kernel': 'poly', 'max_iter': -1, 'shrinking': True, 'tol': 0.001, 'verbose': False
SVRRBF	Hyperparameters: 'C': 5, 'cache_size': 200, 'coef0': 0.0, 'degree': 3, 'epsilon': 0.01, 'gamma': 'scale', 'kernel': 'rbf', 'max_iter': -1, 'shrinking': True, 'tol': 0.001, 'verbose': False
SVRSIGM	Hyperparameters: 'C': 5, 'cache_size': 200, 'coef0': 0.0, 'degree': 3, 'epsilon': 0.01, 'gamma': 'scale', 'kernel': 'sigmoid', 'max_iter': -1, 'shrinking': True, 'tol': 0.001, 'verbose': False
kNN	Hyperparameters: algorithm': 'brute', 'leaf_size': 30, 'metric': 'minkowski', 'metric_params': None, 'n_jobs': None, 'n_neighbors': 3, 'p': 2, 'weights': 'uniform'
DT	Hyperparameters: 'ccp_alpha': 0.0, 'criterion': 'mse', 'max_depth': None, 'max_features': 'sqrt', 'max_leaf_nodes': None, 'min_impurity_decrease': 0.0, 'min_impurity_split': None, 'min_samples_leaf': 1, 'min_samples_split': 2, 'min_weight_fraction_leaf': 0.0, 'random_state': None, 'splitter': 'best'

Table 4: Hyperparameters and attributes of various ML models.

S. No.	Performance metrics	Key equation
1	RMSE	$\mathrm{RMSE}(y,\hat{y})=\sqrt{\frac{1}{n_{\text{samples}}}\sum_{i=1}^{n_{\text{samples}}}(y_i-\hat{y}_i)^2}$
2	MAE	$\mathrm{MAE}(y,\hat{y})=\frac{1}{n_{\text{samples}}}\sum_{i=1}^{n_{\text{samples}}}\lvert y_i-\hat{y}_i\rvert$
3	MAPE	$\mathrm{MAPE}(y,\hat{y})=\frac{1}{n_{\text{samples}}}\sum_{i=1}^{n_{\text{samples}}}\frac{\lvert y_i-\hat{y}_i\rvert}{max(\epsilon,\lvert y_i\rvert)}$
4	R-Square	$\mathrm{R}^2(y,\hat{y})=1-\frac{\sum_{i=1}^{n_{\text{samples}}}(y_i-\hat{y}_i)^2}{\sum_{i=1}^{n_{\text{samples}}}(y_i-\bar{y})^2}$ where $\bar{y}=\frac{1}{n_{\text{samples}}}\sum_{i=1}^{n_{\text{samples}}}y_i$.

Table 5: Model evaluation and performance metrics.

RESULTS AND DISCUSSION

In the results section, a deep analysis of bonded composite repair is shown considering all possible parameter effects. For the first, plate crack length and composite parameters varied for the effect of SIF using an analytical model. Later, analytical model data was compared with the ML algorithms with all parametric effects for the determination of optimal results of SIF.

Comparison of analytical data and ML algorithms

After evaluating the analytical results with all possible parameters, a comparison was made with ML algorithms. The fundamental concepts of fracture parameter-SIF were clearly explained using analytical results [5], and the effects of mechanical properties and dimensions of the composite patch and adhesive bond were demonstrated.

This section presents the results of both analytical and ML algorithms applied to the defined problem. The analytical method utilized a closed-form analytical model based on LEFM and Rose's analytical modelling. Similar studies have been conducted previously [5,36]. The methodologies adopted in this study, including ML algorithms, were considered to address this gap. Different ML techniques were employed to determine optimal results and minimize human efforts. As discussed earlier, each ML algorithm has its advantages and disadvantages. Therefore, this study encompasses a comprehensive approach to optimize SIFs for the present model, utilizing a range of ML techniques.

The fracture behavior of bonded reinforced composites under 1 MPa loading conditions was simulated using analytical modelling and ML algorithms. The objective was to assess the influence of crack length, composite patch, and adhesive bond on the normalized SIF of a center-cracked plate. Fig. 4 and Tab. 6 presents the SIF values of bonded composite patches based on different crack lengths by analytical method and ML techniques. To facilitate comparisons and evaluations, a single table displaying the normalized SIF values of a center-cracked plate bonded to a reinforced composite material was presented, categorized by their corresponding crack lengths. Upon examining the results, it was observed that the maximum reduction in normalized SIF values for cracked aluminium structures occurred at a crack length of 15 mm. Conversely, the minimum reduction in normalized SIF value was obtained for a crack length of 5 mm. The impact of the bonded composite patch increased as the crack length increased from 5 to 15 mm, leading to a decrease in crack propagation. Consequently, the normalized SIF values were lower for larger crack lengths, with a further decrease observed as the crack length increased. The numerical results, which have been validated against benchmark results, are considered the primary findings and are further compared with the analytical and ML algorithms analyses. Although the DT (Decision Tree), OLS (Ordinary Least Squares), and SVR (Support Vector Regression) with the linear kernel (SVRLIN) algorithms generated satisfactory performance values for the normalized SIF, there were some limitations in accurately estimating these parameters. Consequently, these algorithms exhibited some variation in the value of the results in their predictions. It should be noted

that Ridge, Lasso, and Elastic Net algorithms were primarily designed for classification purposes and tend to perform poorly in regression applications.

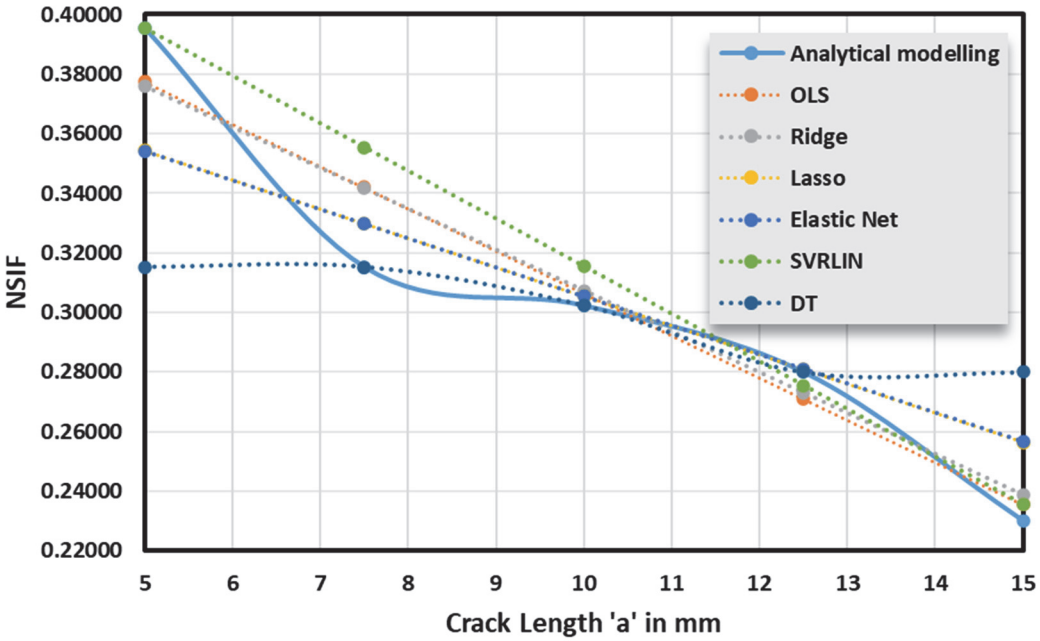

Figure 4: Normalized SIF of the cracked rectangular plate vs crack length.

Crack length 'a' (mm)	Analytical modelling	ML algorithms					
		OLS	Ridge	Lasso	Elastic Net	SVRLIN	DT
5	0.39529	0.37744	0.37587	0.35431	0.35409	0.39528	0.31520
7.5	0.31520	0.34197	0.34157	0.32983	0.32975	0.35536	0.31520
10	0.30229	0.30649	0.30728	0.30537	0.30541	0.31544	0.30228
12.5	0.27995	0.27103	0.27298	0.28089	0.28107	0.27552	0.27994
15	0.23008	0.23555	0.23868	0.25642	0.25674	0.23560	0.27994

Table 6. Normalized SIF of the cracked rectangular plate.

Fig. 5 presents the NSIF values at different data points by analytical and ML models. Fig. 6 presents the observed value of NSIF by analytical model and predicted values of NSIF by various ML models. Tab. 7 presents the normalized SIF values of reinforced composites obtained through convergence methods at a crack length of 10 mm. The study of fracture behavior in reinforcing materials revealed that the thickness of reinforced composites exhibited superior toughness compared to other parameters. Furthermore, the normalized SIFs were influenced by the bonded adhesive layer. Tab. 8 displays the normalized SIFs corresponding to the adhesive bond thickness and shear modulus, obtained through convergence methods at a crack length of 10 mm.

The representations depicting the behavior of repaired structures based on bonded composite parameters and adhesive layer are presented in Tabs. 7 and 8. These tables provide an understanding of the curves associated with all the ML algorithms used in the study. The analytical datasets obtained from the given crack length were utilized for the ML algorithms. While the DT, OLS, and kNN algorithms demonstrated high-performance values in terms of normalized SIFs for the tested crack, their estimation accuracy resulted in some variations in the algorithm outputs. It was observed that Ridge, SVRLIN, SVR with Polynomial (SVRPOLY), and radial basis function (SVRRBF) kernels, primarily designed for classification purposes, produced less satisfactory results in regression applications. Conversely, SVRLIN and SVRPOLY yielded approximately close results. In summary, the addition of reinforced composites to cracked aluminium structures improved the fracture strength of the overall structure when properly adhered.

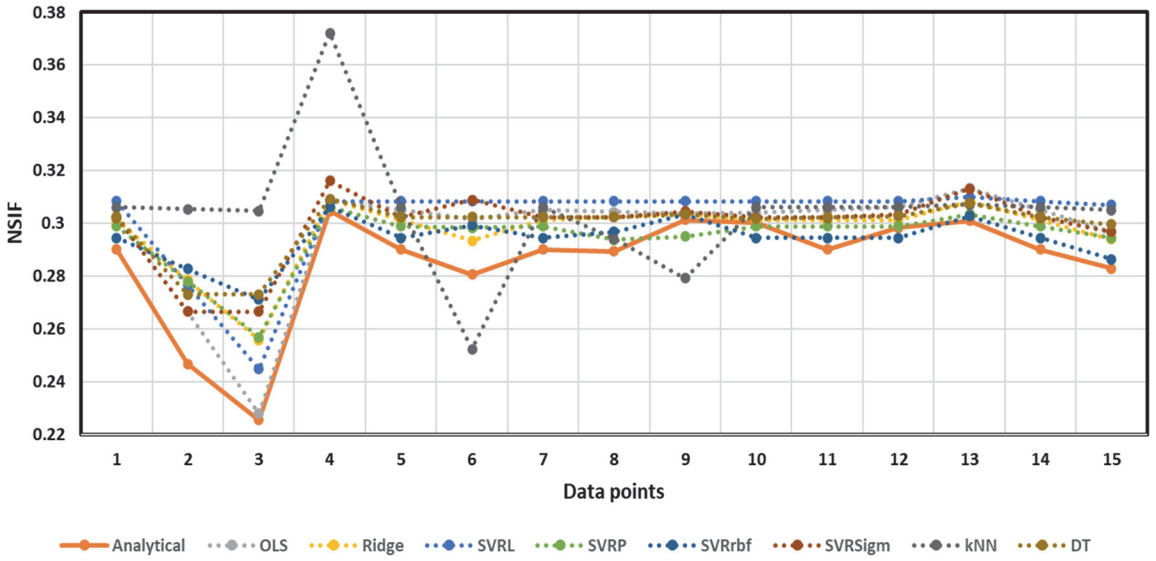

Figure 5: Normalized SIF of the cracked rectangular plate vs crack length for various datapoints.

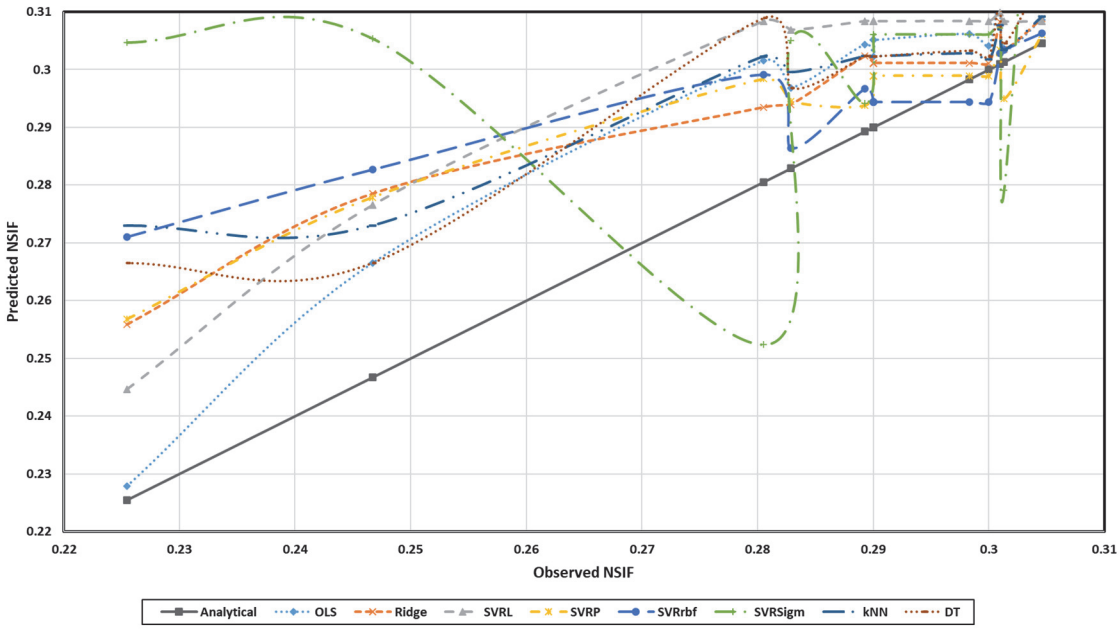

Figure 6: Normalized SIF of the cracked rectangular plate – observed value vs predicted value.

		Patch Dimension (mm)								
		Thickness (Width =20, Height=10)			Width (Thickness =0.5, Height=10)			Height (Thickness =0.5, Width=20)		
Model		0.5	0.75	1	17.5	20	22.5	10	12.5	15
Analytical modelling		0.29003	0.24669	0.22546	0.30458	0.29003	0.2805	0.29003	0.28929	0.30132
ML algorithms	OLS	0.30229	0.2665	0.22792	0.30864	0.30508	0.30152	0.30508	0.30433	0.30357
	Ridge	0.30113	0.27848	0.25582	0.30881	0.30114	0.29346	0.30114	0.30233	0.30352
	SVRLIN	0.30838	0.27653	0.24468	0.30839	0.30839	0.30839	0.30839	0.30839	0.30839
	SVRPOLY	0.29893	0.27787	0.25679	0.30604	0.29893	0.29837	0.29893	0.29379	0.29494
	SVRRBF	0.2944	0.28269	0.27105	0.3063	0.2944	0.29914	0.2944	0.29672	0.30343
	SVRSIGM	0.30611	0.30539	0.30468	0.37211	0.30611	0.25235	0.30611	0.29411	0.27914
	kNN	0.30229	0.27299	0.27299	0.30917	0.30229	0.30229	0.30229	0.30232	0.30345
	DT	0.30228	0.2665	0.2665	0.31605	0.30229	0.30893	0.30229	0.30235	0.30456

Table 7: Effect of composite patch for crack length a = 10mm, adhesive thickness=0.003 mm and shear modulus=1.2 GPa.

Model		Adhesive bond					
		Adhesive Thickness (mm)			Shear Materials (GPa)		
		0.0025	0.003	0.0035	0.6	1.2	1.8
Analytical modelling		0.30001	0.29003	0.29831	0.30098	0.29003	0.28288
ML algorithms	OLS	0.30404	0.30508	0.30612	0.31333	0.30508	0.29683
	Ridge	0.30114	0.30114	0.30114	0.30831	0.30113	0.29396
	SVRLIN	0.30839	0.30839	0.30839	0.30986	0.30838	0.3069
	SVRPOLY	0.29893	0.29893	0.29893	0.30338	0.29893	0.29447
	SVRRBF	0.2944	0.2944	0.2944	0.30277	0.2944	0.28636
	SVRSIGM	0.30611	0.3061	0.306113	0.30716	0.30611	0.30506
	kNN	0.30175	0.30229	0.30279	0.30773	0.30229	0.29956
	DT	0.30228	0.30228	0.30328	0.31317	0.30228	0.29683

Table 8: Effect of adhesive bond for crack length a = 10mm, Patch thickness=0.5 mm, width=20 mm and height= 10mm.

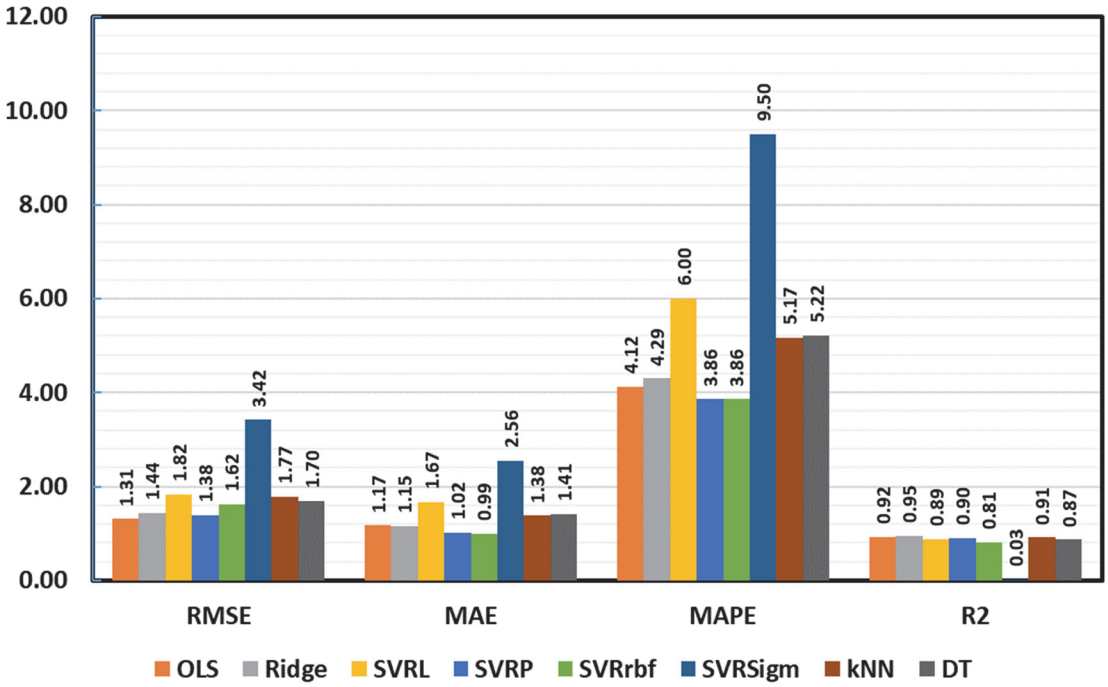

Figure 7: Evaluation metrics for machine learning techniques for crack length a = 10 mm.

Fig. 7 presents the evaluation metrics of various machine learning algorithms. In the figure, the errors values (RMSE, MAE and MAPE) are in percentage. Tab. 9 presents the convergence results of the analytical modelling and ML algorithms in terms of normalized SIF values. These values were reported for different crack lengths that were not experimentally investigated. The model produced normalized SIF values for various crack lengths based on the performance of fracture parameters. The error performance measures, including RMSE, MAE, MAPE, and R^2, were calculated by comparing the FE method with analytical modelling, and these values are presented in Tab. 8. When comparing algorithms, the RMSE, MAE, MAPE, and R^2 metrics are utilized, and Tab. 5 contains the explanations and equations for these metrics. Successful algorithms have lower RMSE, MAE, and MAPE values than other algorithms. The R^2 measure has a range of values from 0 to 1. The closer R^2 is to 1 the better the algorithm's predictions. Each of these measures may be utilized independently to identify the optimal algorithm. From Fig. 7, in terms of RMSE, OLS (0.00434), DT (0.00588), and SVRLIN (0.00669) are the three most successful algorithms. When comparing numerical outcomes by MAE, the three most effective algorithms are DT (0.00197), OLS (0.00322), and SVRLIN (0. 00499), respectively. When looking at the numerical findings for the MAPE metric, the three most effective algorithms are DT (0.00813), OLS (0.01167), and SVRLIN (0.01742), in that order. OLS (0.95641), SVRPOLY (0.95641), and DT (0.94925) are the three most effective algorithms when it comes to R^2 value. To evaluate how the algorithms operate for intermediate values when the numerical results were not tested, the MLA results were compared to the analytical modelling. The R^2 values achieved using MLA are greater than those obtained by the analytical modelling, according to the numerical data. After comparing the algorithms analytically, the SVRRBF and Ridge

algorithms perform poorly in the intermediate value estimation without numerical input. The fact that DT and OLS rank top in all comparisons indicates that this algorithm exceeds the others in terms of regression performance in both numerical and analytical comparisons. But SVMSIGM was the worst-performing algorithm across all metrics in both tests. Indeed, this has been shown by Balcıoglu and Seckin [34].

Machine Learning Model	Evaluation Metrics			
	RMSE	MAE	MAPE	R2
OLS	0.00434	0.00322	0.01167	0.95641
Ridge	0.01316	0.00885	0.03373	0.80159
SVR Linear	0.00669	0.00499	0.01742	0.91120
SVR Poly	0.00750	0.00598	0.02148	0.94653
SVR rbf	0.01726	0.01030	0.03990	0.84763
SVR Sigm	0.02068	0.01272	0.04922	0.07797
kNN	0.00901	0.00564	0.02137	0.94137
DT	0.00588	0.00197	0.00813	0.94925

Table 9. Evaluation metrics for machine learning techniques for crack length a = 10 mm.

The error percentages and convergence coefficients were evaluated in the simulation conducted to compute the normalized SIF values of the isotropic material. The analytical modelling and ML algorithms were employed, and the comparison results are presented in Tab. 10. Previous studies reported a percentage error of up to 9.36% for analytical modelling, whereas the current study demonstrates a percentage error of approximately 4.05%. Hence, the analytical model used in predicting the SIFs of cracked aluminium plates is consistent with prior research. Furthermore, previous investigations on the SIFs of cracked plates using numerical approaches such as analytical modelling and ML algorithms revealed a minimum convergence error of 7.45%. Interestingly, no comparative study was found that combined the analytical modelling and ML algorithms to estimate the SIFs of cracked aluminium plates. Some research employed the correlation coefficient to express the convergence between experimental and predicted results, where an R^2 value of 0.95 is considered the highest correlation coefficient found for calculating and estimating fracture toughness. In this context, the estimated fracture toughness values obtained through the ML algorithms technique exhibit error percentage and correlation coefficient values comparable to those reported in the literature, given the scarcity of SIF values for comparison.

S. No.	Analytical modelling	ML algorithms	R2	References
	Error Percentage (%)			
1	9.36	-	-	Abuzaid et al. [37]
2	-	7.45	0.95	Balcıoglu and Seckin, [34]
3	4.05	7.03	0.95	Current study

Table 10. Comparison of error rates of fracture toughness and SIF values obtained using the FE method, analytical modelling, and ML algorithms.

Conclusion

In conclusion, this study delves into a comprehensive analysis of bonded composite repair, considering a multitude of parameters and employing both analytical modelling and ML algorithms. The investigation focused on the fracture behavior of bonded reinforced composites under loading conditions, specifically examining the normalized SIFs of a center-cracked plate. The results indicated that ML algorithms, particularly DT, OLS, and SVRLIN, demonstrated satisfactory performance in predicting normalized SIFs. The impact of the bonded composite patch on cracked aluminium structures was shown to enhance fracture strength, with the maximum reduction in normalized SIF values observed at a crack length of 15 mm. Additionally, the study explored the effects of composite patch dimensions and adhesive bond properties on SIFs, providing valuable insights into the optimization of bonded composite repairs. Furthermore, the error performance metrics, including RMSE, MAE, MAPE, and R^2, were employed to evaluate the accuracy of the ML algorithms. The results showed that DT, OLS, and SVRLIN exhibited superior performance across various metrics. This work contributes to the bonded composite repair considering a comprehensive analysis that combines analytical modelling and ML techniques. The findings provide guidance for optimizing the design of bonded composite repairs in cracked thin-walled structures.

ACKNOWLEDGEMENT

This research was supported by the Ministry of Education of Malaysia (MOE) through the Fundamental Research Grant Scheme (FRGS/1/2021/TK0/UIAM/01/5). Also, the authors acknowledge the support of the Structures and Materials (S&M) Research Lab of Prince Sultan University.

CONFLICTS OF INTEREST

The authors declare no conflict of interest.

AVAILABILITY OF DATA AND MATERIALS

The datasets used during the current study are available from the corresponding author upon reasonable request.

REFERENCES

[1] Baker, A.A. (1993). Repair Efficiency in Fatigue-Cracked Aluminium Components Reinforced With Boron/Epoxy Patches, Fatigue Fract. Eng. Mater. Struct., 16(7), pp. 753–65, DOI: 10.1111/j.1460-2695.1993.tb00117.x.

[2] Baker, A.A., Rose, L.R.F., Jones, R. (2002). Advances in the bonded composite repair of metallic aircraft structure, Elsevier.

[3] Baker, A. (1999). Bonded composite repair of fatigue-cracked primary aircraft structure, Compos. Struct., 47(1–4), pp. 431–443, DOI: 10.1016/S0263-8223(00)00011-8.

[4] Baker, A.A. (2011). A Proposed Approach for Certification of Bonded Composite Repairs to Flight-Critical Airframe Structure, Appl. Compos. Mater., 18(4), pp. 337–369, DOI: 10.1007/s10443-010-9161-z.

[5] Aabid, A. (2023). Optimization of Reinforcing Patch Effects on Cracked Plates Using Analytical Modeling and Taguchi Design, Materials (Basel)., 16(12), pp. 4348.

[6] Anjum, A., Aabid, A., Hrairi, M. (2023). Analysis of damage control of thin plate with piezoelectric actuators using finite element and machine learning approach, Frat. Ed Integrita Strutt., 66, pp. 112–126, DOI: 10.3221/IGF-ESIS.66.06.

[7] Aabid, A., Ibrahim, Y.E., Hrairi, M. (2023). Optimization of Structural Damage Repair with Single and Double-Sided Composite Patches through the Finite Element Analysis and Taguchi Method, Materials (Basel)., 16(4), pp. 1581.

[8] Baghdadi, M., Serier, B., Salem, M., Zaoui, B., Kaddouri, K. (2019). Modeling of a cracked and repaired Al 2024T3 aircraft plate: Effect of the composite patch shape on the repair performance, Frat. Ed Integrita Strutt., 13(50), pp. 68–85, DOI: 10.3221/IGF-ESIS.50.08.

[9] Li, C., Zhao, Q., Yuan, J., Hou, Y., Tie, Y. (2019). Simulation and experiment on the effect of patch shape on adhesive repair of composite structures, J. Compos. Mater., (100), DOI: 10.1177/0021998319853033.

[10] Aabid, A., Hrairi, M., Ali, J.S.M., Abuzaid, A. (2019). Effect of Bonded Composite Patch on the Stress Intensity Factors for a Center-cracked Plate, IIUM Eng. J., 20(2), pp. 211–221.

[11] Aabid, A., Hrairi, M., Ali, J.S.M. (2020). Optimization of composite patch repair for center-cracked rectangular plate using design of experiments method, Mater. Today Proc., DOI: 10.1016/j.matpr.2020.03.639.

[12] Makwana, A.H., Shaikh, A.A. (2020). Performance assessment and optimization of hybrid composite patch repair of aircraft structure, Multidiscip. Model. Mater. Struct., 16(5), pp. 887–913, DOI: 10.1108/MMMS-03-2019-0052.

[13] Aabid, A., Baig, M., Hrairi, M., Syed, J., Ali, M. (2024). Effect of fiber orientation-based composite lamina on mitigation of stress intensity factor for a repaired plate: a finite element study Abdul, Frat. Ed Integrità Strutt., 68, pp. 209–221, DOI: 10.3221/IGF-ESIS.69.14.

[14] Bouzitouna, W.N., Oudad, W., Belhamiani, M., Belhadri, D.E., Zouambi, L. (2020). Elastoplastic analysis of cracked aluminum plates with a hybrid repair technique using the bonded composite patch and drilling hole in opening mode I,

Frat. Ed Integrita Strutt., 14(52), pp. 256–268, DOI: 10.3221/IGF-ESIS.52.20.
[15] Aabid, A., Hrairi, M., Ali, J.S.M., Sebaey, T.A. (2022). A Review on Reductions in the Stress-Intensity Factor of Cracked Plates Using Bonded Composite Patches, Materials (Basel)., 15(3086), pp. 20.
[16] Ricci, F., Franco, F., Monrefusco, N. (2011).Bonded Composite Patch Repairs on Cracked Aluminum Plates: Theory, Modeling and Experiments. Advances in Composite Materials - Ecodesign and Analysis, pp. 445–464.
[17] Rose, L.R.F. (1988).Theoretical analysis of crack patching. Bonded Repair of Aircraft Structures, pp. 77–106.
[18] Alpaydın, E. (2005). Introduction to Machine Learning .
[19] Radivojac, P., White, M. (2016). Machine Learning Handbook.
[20] Nasiri, S., Khosravani, M.R., Weinberg, K. (2017). Fracture mechanics and mechanical fault detection by artificial intelligence methods: A review, Eng. Fail. Anal., 81(July), pp. 270–293, DOI: 10.1016/j.engfailanal.2017.07.011.
[21] Wang, H., Zhang, W., Sun, F., Zhang, W. (2017). A comparison study of machine learning based algorithms for fatigue crack growth calculation, Materials (Basel)., 10(5), DOI: 10.3390/ma10050543.
[22] Rovinelli, A., Sangid, M.D., Proudhon, H., Ludwig, W. (2018). Using machine learning and a data-driven approach to identify the small fatigue crack driving force in polycrystalline materials, Comput. Mater., 4(1), pp. 1–10, DOI: 10.1038/s41524-018-0094-7.
[23] Balcloğlu, H.E., Seçkin, A.Ç., Aktaş, M. (2016). Failure load prediction of adhesively bonded pultruded composites using artificial neural network, J. Compos. Mater., 50(23), pp. 3267–3281, DOI: 10.1177/0021998315617998.
[24] Atilla, D., Sencan, C., Goren Kiral, B., Kiral, Z. (2020). Free vibration and buckling analyses of laminated composite plates with cutout, Arch. Appl. Mech., 90(11), pp. 2433–2448, DOI: 10.1007/s00419-020-01730-2.
[25] Şimşek, S., Kahya, V., Adıyaman, G., Toğan, V. (2022). Damage detection in anisotropic-laminated composite beams based on incomplete modal data and teaching–learning-based optimization, Struct. Multidiscip. Optim., 65(11), pp. 332, DOI: 10.1007/s00158-022-03421-8.
[26] Eric Reissner. (1947). On Bending of Elas, Q. J. Appl. Math., 5, pp. 55–68, DOI: 10.1090/qam/20440.
[27] Hartranft, R.J., Sih, G.C. (1968). Effect of Plate Thickness on the Bending Stress Distribution Around Through Cracks, J. Math. Phys., 47(1–4), pp. 276–291, DOI: 10.1002/sapm1968471276.
[28] Sih, G.C. (1971). A review of the three-dimensional stress problem for a cracked plate, Int. J. Fract. Mech., 7(1), pp. 39–61, DOI: 10.1007/BF00236482.
[29] Wang, C.H., Rose, L.R.F., Callinan, R. (1998). Analysis of out-of-plane bending in one-sided bonded repair, Int. J. Solids Struct., 35(14), pp. 1653–1675, DOI: 10.1016/S0020-7683(97)00129-7.
[30] Tada, H., Paris, P.C., Irwin, G.R. (2000). The Stress Analysis of Cracks Handbook, Third Edition, DOI: 10.1115/1.801535.
[31] Rose, L.R.F., Wang, C.H. (2002). Analytical Methods for Designing Composite Repairs, Adv. Bond. Compos. Repair Met. Aircr. Struct., 1–2, pp. 137–175, DOI: 10.1016/B978-008042699-0/50009-7.
[32] Wang, H.T., Wu, G., Pang, Y.Y. (2018). Theoretical and numerical study on stress intensity factors for FRP-strengthened steel plates with double-edged cracks, Sensors (Switzerland), 18(7), DOI: 10.3390/s18072356.
[33] Aabid, A., Hrairi, M., Abuzaid, A., Mohamed Ali, J.S. (2021). Estimation of stress intensity factor reduction for a center-cracked plate integrated with piezoelectric actuator and composite patch, Thin-Walled Struct., 158, DOI: 10.1016/j.tws.2020.107030.
[34] Balcıoğlu, H.E., Seçkin, A.Ç. (2021). Comparison of machine learning methods and finite element analysis on the fracture behavior of polymer composites, Arch. Appl. Mech., 91(1), pp. 223–239, DOI: 10.1007/s00419-020-01765-5.
[35] Pedregosa, F., Weiss, R., Brucher, M., Varoquaux, G., Gramfort, A., Michel, V., Thirion, B., Grisel, O., Blondel, M., Prettenhofer, P., Weiss, R., Dubourg, V., Vanderplas, J., Passos, A., Cournapeau, D., Brucher, M., Perrot, M., Duchesnay, É. (2011). Scikit-learn: Machine Learning in Python, J. Mach. Learn. Res., 12(85), pp. 2825–2830.
[36] Aabid, A., Hrairi, M., Abuzaid, A., Syed, J., Ali, M. (2021). Estimation of stress intensity factor reduction for a center-cracked plate integrated with piezoelectric actuator and composite patch, Thin-Walled Struct., 158, pp. 107030, DOI: 10.1016/j.tws.2020.107030.
[37] Abuzaid, A., Hrairi, M., Dawood, M.S. (2018). Experimental and numerical analysis of piezoelectric active repair of edge-cracked plate, J. Intell. Mater. Syst. Struct., 29(18), pp. 3656–3666, DOI: 10.1177/1045389X18798949.